Article

Not peer-reviewed version

Decadal Stability and Trends in the Global Cloud Amount and Cloud Top Temperature in the Satellite-Based Climate Data Records

Abhay Devasthale * and Karl-Göran Karlsson

Posted Date: 23 June 2023

doi: 10.20944/preprints202306.1668.v1

Keywords: Clouds; Remote Sensing; Climate change; Climate Data Records; Essential Climate Variables; Cloud properties; Stability and trends

Article

Decadal Stability and Trends in the Global Cloud Amount and Cloud Top Temperature in the Satellite-Based Climate Data Records

Abhay Devasthale * and Karl-Göran Karlsson

Meteorological Research Unit, Research and Development, Swedish Meteorological and Hydrological Institute (SMHI), Folkborgvägen 17, 60176 Norrköping, Sweden

* Correspondence: abhay.devasthale@smhi.se

Abstract: 40 years of cloud observations are available globally from satellites allowing derivation of climate data records (CDRs) for climate change studies. The aim of this study is to investigate how stable these cloud CDRs are and whether they qualify stability requirements recommended by the WMO's Global Climate Observing System (GCOS). We also investigate robust trends in global total cloud amount (CA) and cloud top temperature (CTT) that are significant and common across all CDRs. The latest versions of four global cloud CDRs, namely CLARA-A3, ESA Cloud CCI, PATMOS-x and ISCCP-HGM, are analysed. This assessment finds that all three AVHRR based cloud CDRs satisfy even the strictest GCOS stability requirements for CA and CTT when averaged globally. While CLARA-A3 is most stable in global averages, PATMOS-x offers the most stable CDR spatially. While we find these results highly encouraging, there however remain large spatial differences in the stability of and across the CDRs. All four CDRs continue to agree on the statistically significant decrease in global cloud amount over the last four decades, although this decrease is now weaker compared to the previous assessments. This decreasing trend is stabilizing or even reversing in the last two decades; the latter is seen also in MODIS-Aqua and CALIPSO GEWEX datasets. Statistically significant trends in CTT are observed in global averages in the AVHRR-based CDRs, but the spatial agreement in the sign and the magnitude of the trends is weaker compared to those in CA. We also present maps of Common Stability Coverage and Common Trend Coverage that could provide a valuable metric to carry out an ensemble-based analysis of the CDRs.

Keywords: clouds; remote sensing; climate change; climate data records; essential climate variables; cloud properties; stability and trends

1. Purpose and aims

At the planetary scale, clouds provide much-needed cooling umbrella to make our planet bearable and habitable. Without those roughly 20 W/m2 of radiation that clouds cool off at the surface globally and without their cohesive role in regulating the other atmospheric components not least the precipitation, our Earth System would enter into an entirely new paradigm that is best left to our imagination. It is therefore unsurprising that the role of clouds often takes a center stage when discussing current and future climate change and feedbacks [1–12]. Clouds are however notoriously difficult to represent in climate models due to their multifaceted radiative and dynamical effects and they are often pointed out as the reasons behind uncertainties in climate models and the estimated spread in the Earth's equilibrium climate sensitivity [13–28]. It is therefore only justifiable that one of the Grand Challenges listed by the World Climate Research Programme deals with improving our holistic understanding of clouds, circulation and climate sensitivity (https://www.wcrp-climate.org/gc-clouds).

Cloud observations from meteorological satellites are available since the late 1970s Due to their multidecadal and near uniform data records, now spanning 40 years, these satellite-based observations of cloud properties provide important insights and constraints on to our understanding

of clouds. From the pioneering and ground-breaking work done in the framework of International Satellite Cloud Climatology Project since the early 1980s [29,30], the enormous progress made by the NOAA's flagship Pathfinder Program through their PATMOS-x data records [31], to the dedicated and continuous developments in the frameworks of EUMETSAT's Satellite Application Facility on Climate Monitoring (CM-SAF) [32,33] as well as ESA's recent Climate Change Initiative [34], the cloud climate data records (CDRs) from these various efforts have unraveled many new insights into the role of clouds in climate. As pointed out by many studies, the recent improvements in and the maturity of these CDRs are mainly attributed to the novelties and capabilities of NASA's Afternoon-Train sensors such as Moderate Resolution Imaging Spectroradiometer (MODIS) onboard Aqua satellite [35], Cloud-Aerosol Lidar with Orthogonal Polarization (CALIOP) onboard Cloud-Aerosol Lidar and Infrared Pathfinder Satellite Observations (CALIPSO) and Cloud Profiling Radar (CPR) onboard CloudSat [36].

The cloud CDRs are requested to follow certain accuracy and stability standards. This is especially important if a cloud CDR is to be used to detect a physical climate trend or a climate change signal that is free from potential technical and sampling artifacts. Each cloud CDR usually undergoes robust evaluation and scientific validation iteratively. While the uncertainties and biases in the cloud CDRs are documented regularly, very little is known about their decadal stability and robust trends that are common across all CDRs. The aim of this study is to assess those two aspects. The work presented here on the stability assessment is unprecedented and never been attempted before in such detail. Furthermore, this study provides an update to the last assessment of cloud CDRs done five years ago by Karlsson and Devasthale (2018) in the framework of CM-SAF [37] and about a decade ago by Stubenrauch et al. (2013) in the framework of GEWEX Cloud Assessment [38]. The evaluation of common and robust trends in global cloud amounts and cloud top temperatures in the latest versions of CDRs is also novel.

2. Satellite based cloud data records

In this study we evaluated four cloud climate data records that span over more than 35 years. The first CDR is the third edition of the CM SAF cLoud, Albedo and surface RAdiation dataset from AVHRR data, CLARA-A3 [39]. The Level 3 monthly mean cloud products available at 0.25 degree grids are used. The AVPOS flavour of this dataset, providing monthly means based on all available, quality-controlled data from AVHRRs onboard different satellites, is analysed here. The CLARA-A3 CDR currently covers the period from 1979 to 2020 with Interim CDR thereafter. The second CDR used here is derived in the framework of ESA's Climate Change Initiative. It provides L3 monthly mean cloud properties from AVHRRs based on afternoon prime NOAA satellites at 0.5 degree grids and covers the period from 1982 to 2018. The latest Version 3 CDR is used [40]. The third CDR used here, PATMOS-x V06r00, is provided by NOAA with its heritage in the flagship Pathfinder program [41]. It provides cloud properties at 0.1 deg grids and covers the period from 1982 to 2020. We used daily mean L2b PATMOS-x data and computed L3 monthly means in the same way as is done in CLARA-A3. The fourth CDR used here is provided in the framework of International Satellite Cloud Climatology Project (ISCCP). The ISCCP-HGM CDR (v01r00) is available from 1983 through June 2017 and a corresponding ICDR thereafter through Dec 2018 [42].

In addition to the CDRs, we used monthly mean cloud products from MODIS-Aqua (MYD08 Version 6 product) [35]. MODIS-Aqua provides nearly 20 years of uniform cloud property data starting from 2002 and due to its orbital and calibration stability (see an overview in [43]) can be considered the most suitable independent reference to test the stability of the four CDRs mentioned above.

 doi:10.20944/preprints202306.1668.v1

3. Stability assessment of global cloud CDRs

3.1. A global overview of stability

Here, the stability of global cloud amount and cloud top temperature is evaluated against the requirements set by the WMO Global Climate Observing System (GCOS) [44]. These requirements are given in Table 1. Stability of a climate variable is defined here as the change in bias over time as stipulated in GCOS-245 [44]. The biases are computed against an independent stable reference which is MODIS-Aqua in our case. It is to be noted that the requirements set by GCOS are even stricter than those set by CM-SAF. In their most recent implementation plan [44], GCOS provides three levels of requirements termed as Threshold, Breakthrough and Goal, the last one being the strictest. Different regions on the globe can satisfy different levels of stability requirements. In the most ideal case, it is recommended that the Goal requirements are satisfied by a climate variable, but the Breakthrough requirements are also acceptable for climate studies depending on the application. The regions where even the Threshold requirements are not satisfied, detecting a climate change signal that is free from potential satellite artifacts is very difficult.

Table 1. Stability requirements recommended by the WMO's GCOS (GCOS-245, 2022).

Requirement level	CA (% per decade)	CTT (K per decade)
Goal	0.3	0.2
Breakthrough	0.6	0.4
Threshold	1.2	0.8

We first present an overview of stability at a global scale in Figures 1 and 2 for the cloud amount and cloud top temperature respectively. The subplots in these figures show biases against MODIS-Aqua and the fitted trends therein. All four CDRs show seasonality in the cloud amount biases against MODIS (Figure 1), which can be explained by the different detection sensitivity of these CDRs and the seasonal differences in the monsoonal systems and inter-tropical convergence zones between the two hemispheres (see [45,46] for further details). It is to be noted that all AVHRR based CDRs (i.e. CLARA-A3, ESA Cloud CCI and PATMOS-x) satisfy even the strictest GCOS Goal requirements on the stability of derived cloud amounts. The best stability is observed in CLARA-A3 dataset when averaged globally. The ISCCP-HGM series however does not satisfy the GCOS requirements. The ISCCP-HGM retrieval algorithms are being unfairly punished by the fact that they have to use the least common denominator set of channels while harmonizing the data from the polar and geostationary satellites and that they have varying sampling throughout the observational period. These aspects seem to be affecting the cloud detection sensitivity varyingly over time, resulting in stronger trends in the biases.

Figure 2 shows the stability of global mean cloud top temperatures in the four CDRs. In this case as well all three AVHRR based CDRs satisfy even the strictest GCOS requirements, while the ISCCP-HGM series fails to do so for the same reasons mentioned above. It is to be noted as well that, as expected, the absolute CTT biases in the CLARA-A3 and PATMOS-x CDRs are high. This is mainly due to a) the different selection of Level 2 to Level 3 clouds (e.g. MODIS doesn't include broken cloudiness in L3 cloud top products), and b) the improved and rigorous training of optimal estimation and artificial neural network algorithms using CALIPSO to improve the detection and placement of clouds in PATMOS-x and CLARA-A3 in the recent years [39,41,47].

Preprints (www.preprints.org) | NOT PEER-REVIEWED | Posted: 23 June 2023 doi:10.20944/preprints202306.1668.v1

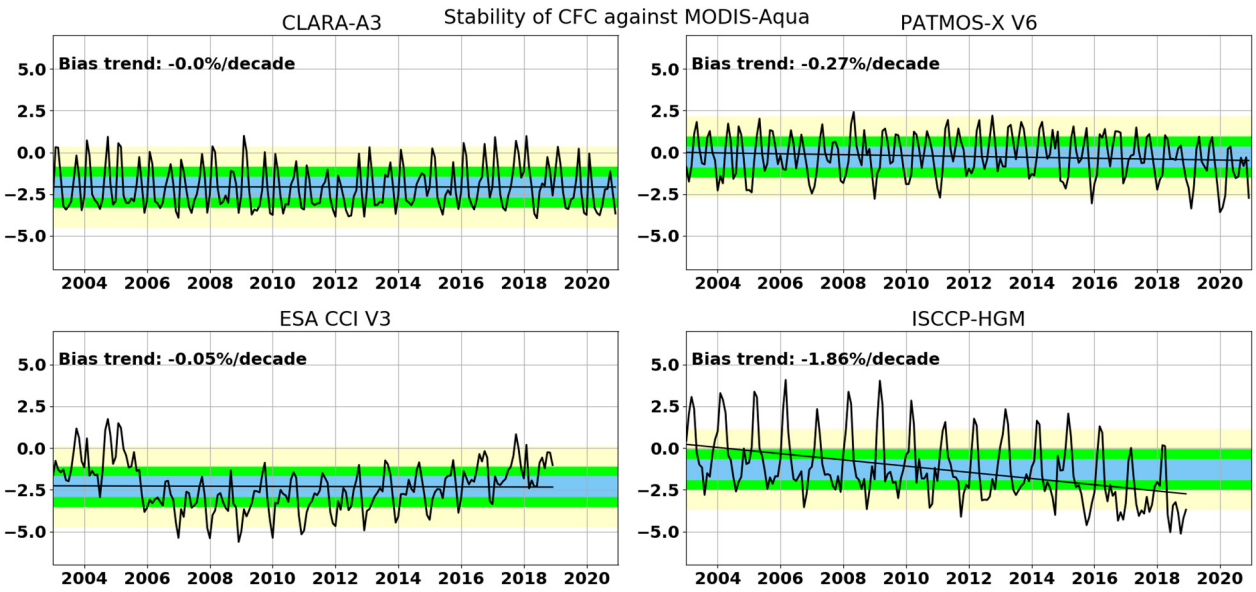

Figure 1. Stability of global mean total cloud amount. The monthly mean biases against MODIS-Aqua are shown together with trends in the bias. The blue, green and yellow envelopes show the goal, breakthrough and threshold stability requirement recommended by the WMO's GCOS. .

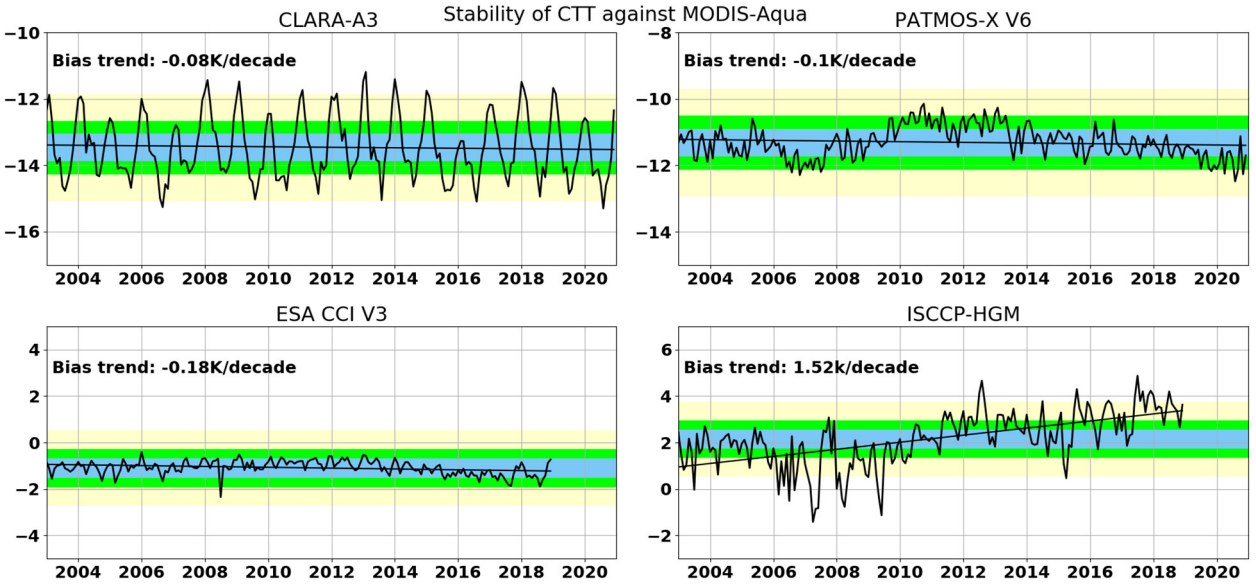

Figure 2. Same as in Figure 1, but for cloud top temperature.

3.2. Reginal features of stability

The cloud detection sensitivity and the accuracy of retrieval algorithms varies regionally and they could also be cloud regime dependent. We therefore investigated the spatial patterns of stability as shown in Figures 3 and 4 for the cloud amount and cloud top temperature respectively. Figures 3 and 4 indeed show strong regional features in the stability of cloud amount and CTTs.

Preprints (www.preprints.org) | NOT PEER-REVIEWED | Posted: 23 June 2023 doi:10.20944/preprints202306.1668.v1

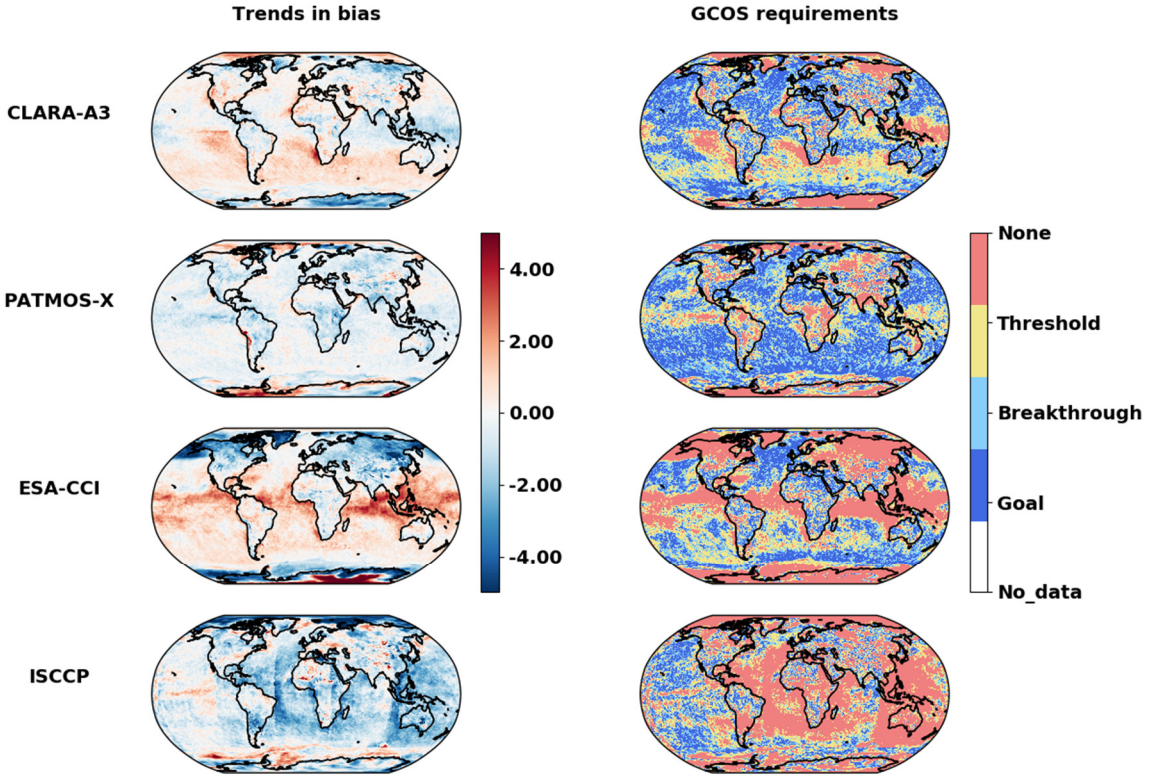

Figure 3. Spatial patterns of the stability of cloud amount (% per decade, left column) and the right column shows which regions satisfy the GCOS stability requirements in question.

Preprints (www.preprints.org) | NOT PEER-REVIEWED | Posted: 23 June 2023 doi:10.20944/preprints202306.1668.v1

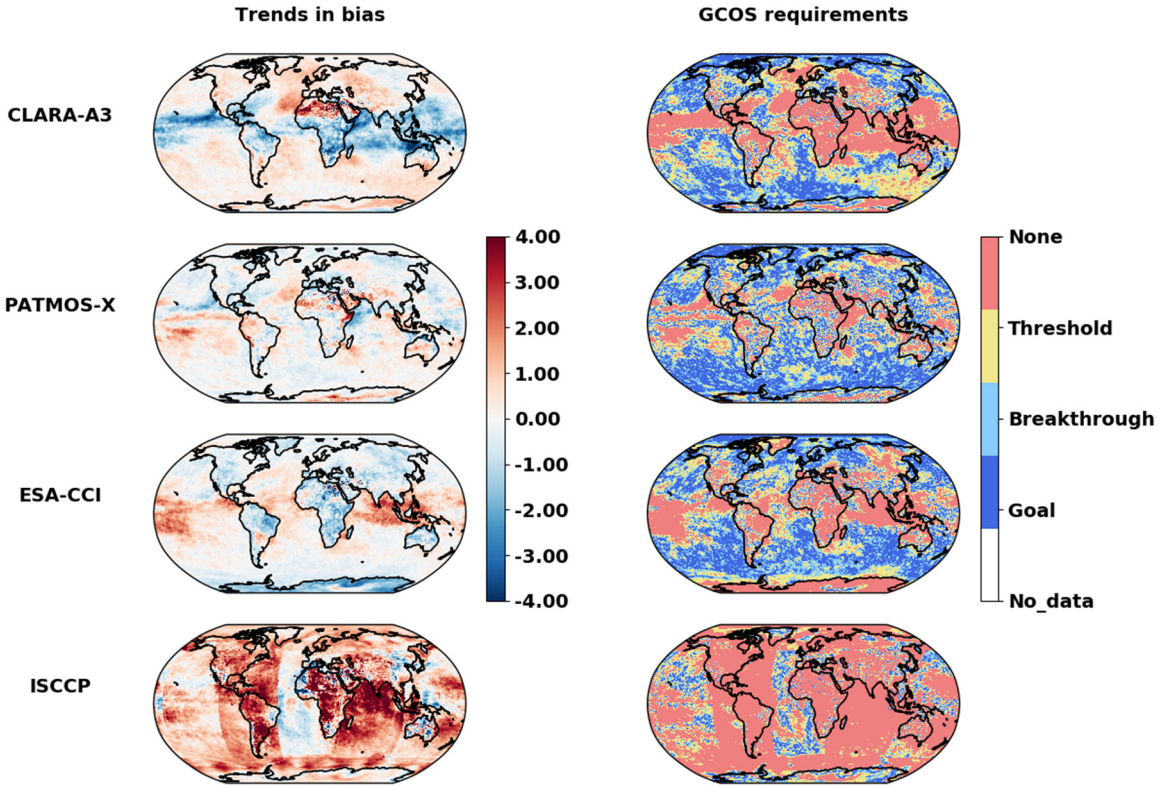

Figure 4. Spatial patterns of the stability of cloud top temperature (K per decade, left column) and the right column shows which regions satisfy the GCOS stability requirements in question.

Over the majority of the Earth's surface, CLARA-A3 and PATMOS-x satisfy the Breakthrough and Goal requirements for cloud amount (Figure 3). The strongest trends in the CA biases are observed over the polar regions, Pacific warm pool and the southern hemispheric sub-tropical and mid-latitude regions in CLARA-A3. In the PATMOS-x CDR the strongest trends in biases are observed also over the polar regions and over the parts of the ITCZ. Compared to the AVHRR based CLARA-A3 and PATMOS-x versions of CDRs used here, the ESA Cloud CCI CDR has more pronounced trends in the biases and there is a clear zonal gradient evident. These features and differences in the bias trends can be explained by the fact that ESA Cloud CCI uses data from only prime NOAA satellites, thus making it more vulnerable to the impacts of orbital drift of NOAA satellites [48]. On the other hand, the CLARA-A3 and PATMOS-x versions used here are based on all available quality-controlled data from different NOAA and MetOp platforms, making them less sensitive to such impacts. The ISCCP-HGM CDR satisfies the GCOS requirements over the Pacific Ocean and the parts of Southern Ocean, Eurasia and Indian Ocean. It does however show spatial artifacts associated with the edges of the geostationary discs and the non-uniform sampling [49]. Overall the cloud amounts from the PATMOS-x CDR performs best regionally while satisfying the Goal, Breakthrough and Threshold requirements.

Figure 4 further reveals interesting spatial features in the stability of CTTs. The negative trends in the CTTs biases in the CLARA-A3 CDR are high in the ITCZ regions and, as a result, it does not satisfy the GCOS requirements over those regions. In the mid-latitude regions, the trends in the biases are positive and weaker and satisfy the requirements. The ESA Cloud CCI CDR also shows the similar features. The artifacts in the ISCCP-HGM CDR are even more visible in the CTT bias trends than in the cloud amounts. All three AVHRR based CDRs satisfy the strictest stability requirements over the

Preprints (www.preprints.org) | NOT PEER-REVIEWED | Posted: 23 June 2023 doi:10.20944/preprints202306.1668.v1

Southern Oceans, and the northern and southern parts of the Pacific Ocean. The PATMOS-x CTT CDR shows the best agreement with the GCOS requirements regionally.

A user-friendly synthesis of all stability results together is presented in Figure 5. It shows the common stability coverage (CSC), i.e. the geographical areas that are common across different combinations of CDRs where they satisfy at least the Threshold GCOS stability requirements for cloud amount and CTT. Since the absolute cloud amounts in CLARA-A3 and PATMOS-x are closest to one another, their CSC is also globally largest. With each subsequent addition of another CDR, first ESA Cloud CCI and then ISCCP-HGM, the CSC decreases as the disagreements among the CDRs also increase. The areas where all four CDRs have CSC include the parts of northern and southern Pacific Ocean, parts of Southern Oceans, and northern North Atlantic Ocean. They also have CSC over some of the land regions, such as central Europe, parts of continental USA, parts of Amazonia and the African continent. The spatial features in the CSC of CTTs are similar to those features observed for cloud amounts over the oceanic areas. However, over the land regions, the CSC of CTTs is very small among all four CDRs.

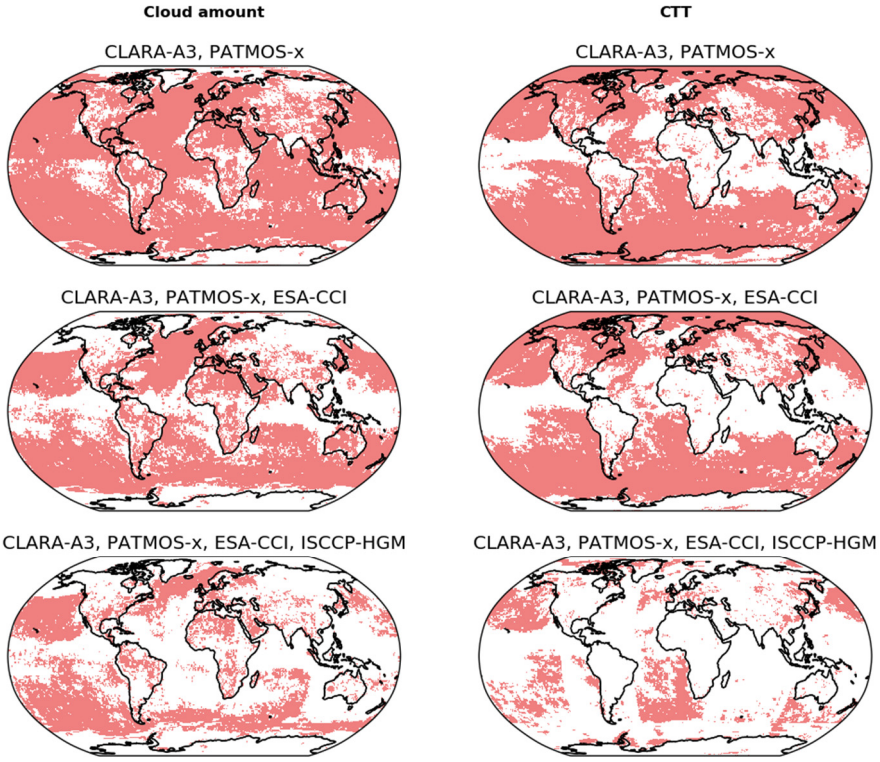

Figure 5. Common Stability Coverage (CSC) for cloud amount (left column) and cloud top temperature (right column) showing the regions where different combinations of the cloud CDRs simultaneously satisfy at least the threshold requirements recommended by the GCOS.

4. Robust trends in global CA and CTT

4.1.1. A global overview of trends

Having assessed the stability of cloud CDRs, we investigate next the global trends in these CDRs and the robustness of these trends across them. Figure 6 and Figure 7 show the deseasonalized anomalies of CA and CTT respectively based on the four CDRs in question. The shorter time-series from MODIS-Aqua and two flavours of GEWEX-like cloud products from CALIOP-CALIPSO (Top Layer and Passive) are also shown for comparison. All four cloud CDRs show a statistically

Preprints (www.preprints.org) | NOT PEER-REVIEWED | Posted: 23 June 2023 doi:10.20944/preprints202306.1668.v1

significant decreasing trend in CA over the last 40 years (Figure 6), although the magnitude of this trend is different among the CDRs. A stabilization of this trend or even a reversal is seen in the last two decades, also seen in MODIS-Aqua and CALIPSO. The inter-annual variability in the total CA remains within few percentage points in all CDRs.

There are many potential reasons why different CDRs have different magnitude of trends and why the interannual variability in them is also different. It is to be noted that we have learned many lessons since the comprehensive assessment of cloud property datasets derived from satellite sensors was first done in the framework of GEWEX Cloud Assessment [38]. For example, we have a better understanding of the cloud detection sensitivity (CDS), which is different among different CDRs. The CDS itself depends on the retrieval algorithm used (e.g. probabilistic naïve Bayesian versus hierarchical threshold based), the number of detection features and threshold used, the training datasets, handling of multilayer clouds, reanalysis and surface data used etc. The different programmatic nature of these CDRs is also to be noted. For example, while ISCCP-HGM is based on the amalgamation of data from sensors onboard various geostationary and polar orbiting satellites, the other three CDRs are primarily based on AVHRR sensors onboard polar orbiting NOAA and MetOp satellites (except PATMOS-x, the newest version of which also ingests information from HIRS sensors onboard the same polar orbiting satellites). While all three AVHRR-based CDRs have nearly identical calibration, ISCCP-HGM has a different approach. Furthermore, ESA CCI Cloud CDR is based only on prime satellites, while CLARA-A3 and PATMOS-x versions used here are based on quality controlled AVHRR data from all available NOAA and MetOp satellites. Different approaches to convert Level 2 swath-based products into Level 3 monthly means also contribute to the observed differences. Given these large programmatic, algorithmic, and configurational differences among the cloud CDRs, we find it highly encouraging that these CDRs are converging towards one another over the years and that all of them agree on a robust decreasing trend in the CA in global averages.

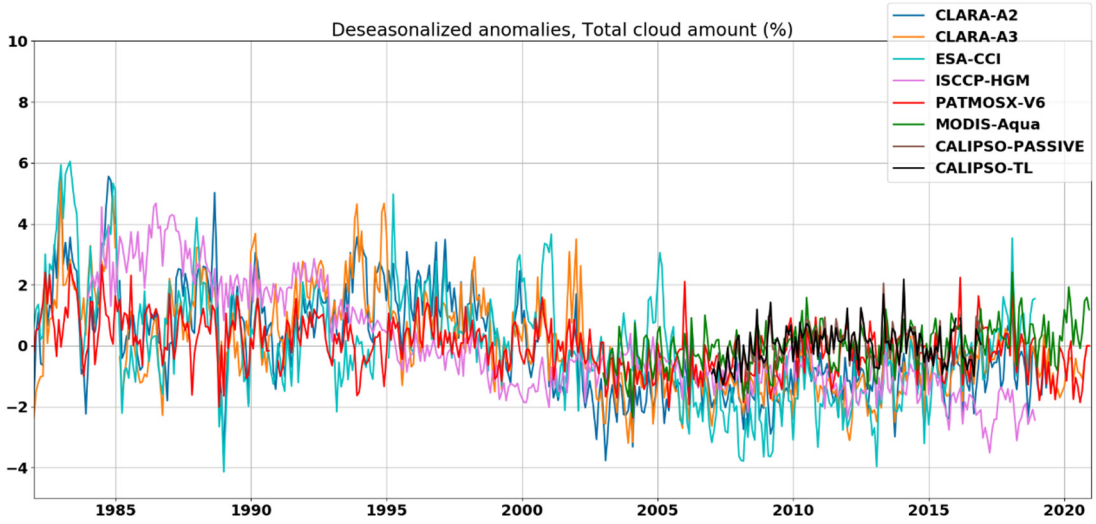

Figure 6. Deseasonalized anomalies of global mean total cloud amount (%) derived from four cloud CDRs as well as from MODIS-Aqua and CALIPSO. The trends in CLARA-A3, PATMOS-x, ESA-CCI, ISCCP-HGM are -0.76%, -0.28%, -0.82% and -1.47% per decade respectively. All trends are statistically significant based on Mann Kendall test.

Figure 7 shows deseasonalized global mean cloud top temperatures. CLARA-A3 and PATMOS-x show statistically significant cloud top cooling, while ESA Cloud CCI shows significant warming of the cloud tops. The trend in ISCCP-HGM is very weak and not statistically significant. The interannual variability in the CDRs is strong in the first 20 years. It is difficult to understand if this is a physical feature or an artifact. It is to be noted that these years are marked by strong volcanic eruptions (El Chichon in 1983, Pinatubo in 1991) as well as many strong El Nino/La Nina events. In

Preprints (www.preprints.org) | NOT PEER-REVIEWED | Posted: 23 June 2023 doi:10.20944/preprints202306.1668.v1

the recent 20 years, the interannual variability in CTTs is weaker and the majority of the data records, including MODIS and CALIPSO, show cloud top warming.

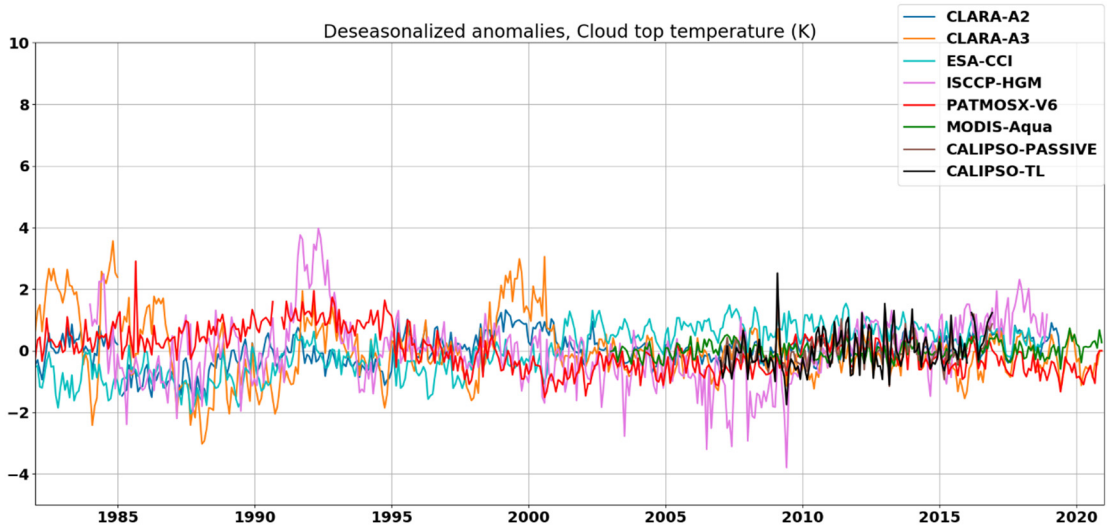

Figure 7. Deseasonalized anomalies of global mean cloud top temperature (K) derived from four cloud CDRs as well as from MODIS-Aqua and CALIPSO. The trends in CLARA-A3, PATMOS-x, ESA-CCI, ISCCP-HGM are -0.17, -0.32, 0.56 and 0.055 Kelvin per decade respectively. All trends are statistically significant except in the case of ISCCP-HGM.

4.1.2. Regional trends in CA and CTT

Over which regions of the Earth the CDRs agree in trends? Figures 8 and 9 provide information to answer this question by showing not only the decadal trends in the individual CDRs, but also by showing the common trend coverage (CTC). The CTC shows the common regions where the CDRs agree on either increasing or decreasing trends as well as the regions where they either don't agree or the trends are not statistically significant. While interpreting these spatial trends in the CDRs, it is important to keep in mind the programmatic, algorithmic and configurational differences in the CDRs mentioned before. Here, we focus only on the CDRs that are predominantly AVHRR-based. The ISCCP-HGM does not satisfy the GCOS stability requirements and shows artifacts associated with the geostationary discs and therefore likely not suitable for studying spatial trends (see Figures 3-5).

Preprints (www.preprints.org) | NOT PEER-REVIEWED | Posted: 23 June 2023 doi:10.20944/preprints202306.1668.v1

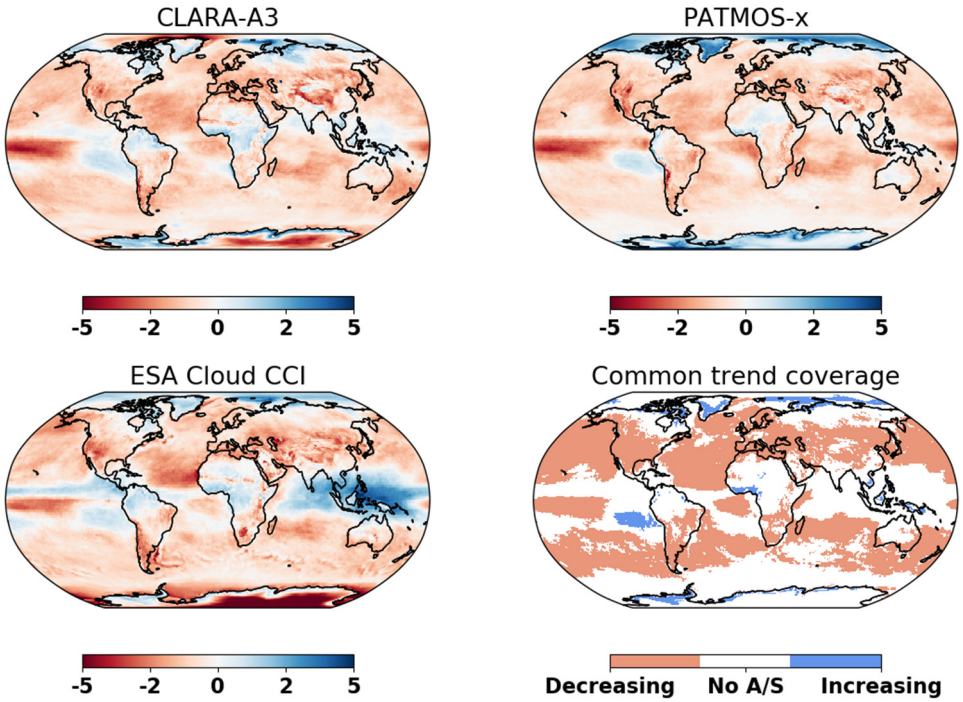

Figure 8. Trends in total cloud amount (%/decade) in the three predominantly AVHRR-based CDRs. The Common Trend Coverage (CTC) shows the regions where all three CDRs simultaneously show either increasing or decreasing trends that are statistically significant. The while areas in CTC show the regions where the CDRs either don't agree on the sign of the trend or the trend is insignificant.

The CTCs for cloud amount reveal interesting features regionally (Figure 8). For example, there is a good agreement in the CA trends among the three AVHRR-based CDRs in the sub-tropical and mid-latitude regions in both hemispheres, where they show a large-scale decrease in the total cloudiness. The CA decrease is stronger over the oceanic regions over these latitudes compared to the land regions. Another interesting feature is the increasing trend in CA in the Arctic, which is driven mainly by the increasing cloudiness over the regions where the sea-ice is decreasing rapidly during and just after the annual melt season in the autumn. A third interesting feature is the increasing cloudiness off the northwestern coast of South America. All three CDRs agree on the statistically significant increasing trend in this region. While this region is strongly affected by the interannual variability associated with El Nino Southern Oscillation, it is important to note that the studies have shown long-term cooling trends in the sea-surface temperatures over this region. This can partly explain the increasing cloudiness as the cooler SSTs favour cloud maintenance.

Preprints (www.preprints.org) | NOT PEER-REVIEWED | Posted: 23 June 2023 doi:10.20944/preprints202306.1668.v1

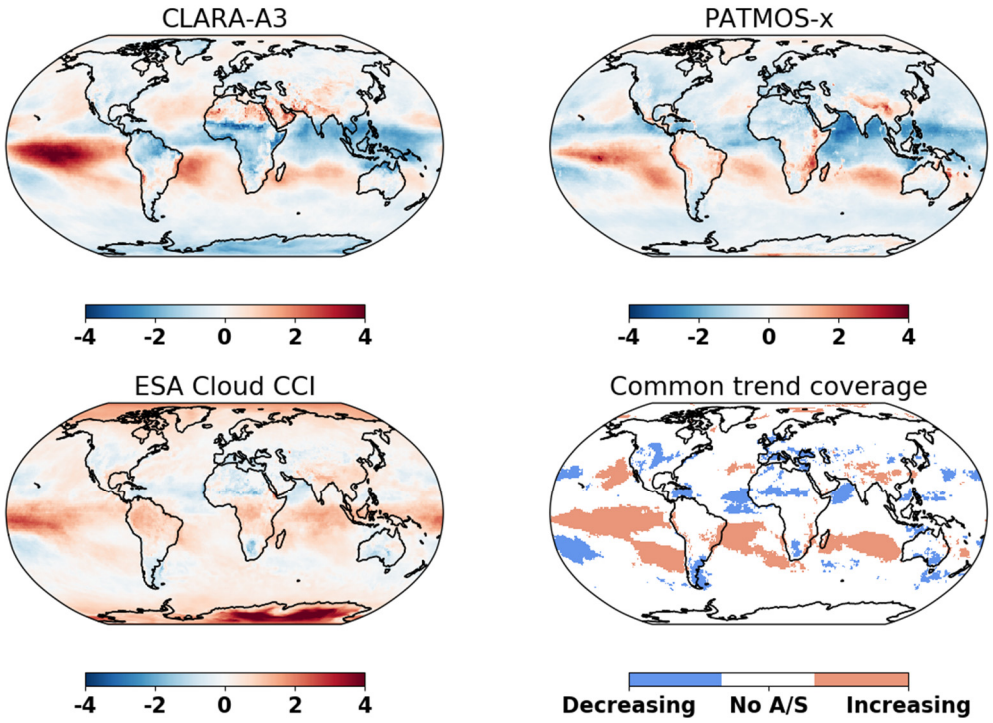

Figure 9. Same as in Figure 8, but for cloud top temperature. The trends are in Kelvin per decade.

The cloud amount trends in the tropical convective regions are difficult to interpret. While CLARA-A3 and PATMOS-x agree on decreasing cloudiness over the tropical Indian and Atlantic Oceans, ESA Cloud CCI however shows increasing trends in the tropical Indian Ocean and also to some extent in the Atlantic. Over the tropical warm pool region in the Pacific, ESA CCI has the strongest increasing trend. While CLARA-A3 and PATMOS-x also show a slight (statistically insignificant) increase over and around Indonesia, further away from the islands, these two CDRs show a large-scale decrease, albeit very small in magnitude. It is to be noted here that while ESA CCI Cloud CDRs uses data from only prime satellites, the CLARA-A3 and PATMOS-x flavours of CDRs used here are based on data from all available satellites. This makes the ESA CCI Cloud CDR more sensitive to the effects of orbital drift, especially in the tropics where the diurnal cycle of convection and associated clouds is stronger compared to mid- and high latitude clouds. Furthermore, the thin cirrus detection sensitivity of CLARA-A3 and PATMOS-x is expected to be better compared to ESA Cloud CCI retrieval algorithm due to rigorous training and constraints based on CALIPSO data in these two CDRs in the recent data processing rounds. These aspects can partly explain the observed differences in trends in these three CDRs over the tropical regions. In the tropical central Pacific, just below the equator, all three CDRs show a strong decrease in cloudiness. In fact, this decrease is strongest among all oceanic regions. A similar agreement in decreasing cloudiness is also observed in the central Atlantic, just off the western coast of Africa (Cape Verde Basin) and in the Gulf of Guinea (Guinea Basin).

The trends in CA over the Southern Oceans, especially over the open waters near the Antarctica, are very weak in CLARA-A3 and PATMOS-x. In a cautionary note, the users are strongly advised to use the clouds CDRs carefully in the Antarctic regions as the uncertainties in the CDRs remain very high, especially during the polar winters.

Figure 9 shows that the CTC for cloud top temperature is considerably limited spatially compared to the CTC for cloud amount. In general, all three CDRs show increasing cloud top temperatures over the regions where these CDRs agree with regard to large-scale decreases in cloudiness (Figure 8). But over the majority of the regions, the CDRs either don't agree or the trends are very weak and statistically insignificant. A closer inspection of the CDRs shows that CLARA-A3 and PATMOS-x agree the most with one another, especially in the tropics. For example, both of these

CDRs show a significant increase in cloud top temperatures in the central-eastern Pacific southern Atlantic Ocean and southern Indian Ocean. They also show statistically significant increase in cloud top temperatures over the tropical warm pool and northern Indian Ocean, including the Arabian Sea and Bay of Bengal. Over the land regions, the trends in CTTs are quite weak, especially in the northern hemisphere.

5. Conclusions

A detailed stability assessment of the satellite-based cloud climate data records was carried out for the first time. Such an assessment was overdue, given that the CDRs are now covering the last 40-years enabling climate change studies. The stability is defined as the trend in bias against the reference, in our case MODIS-Aqua. We evaluated two climate variables, namely total cloud amount and cloud top temperature.

We report that, when averaged globally, the predominantly AVHRR-based cloud CDRs (i.e. CLARA-A3, ESA Cloud CCI V3 and PATMOS-x V6) satisfy even the strictest requirements recommended by the WMO's Global Climate Observing System. CLARA-A3 offers the most stable CDRs in global averages. A closer inspection of the spatial patterns of stability however reveals that PATMOS-x offers the most stable CDRs spatially. We find it very encouraging that the AVHRR-based CDRs are converging towards one another and are extremely stable in global averages in spite their algorithmic and programmatic differences. We also however note that all CDRs show strong spatial variability in the stability and there are still many regions on Earth where the CDRs do not satisfy even the most relaxed GCOS requirements. These conclusions apply to both cloud amount and cloud top temperature.

Compared to the previous assessments, the global decrease in cloud amount in the recent versions of the CDRs is weaker, but still statistically significant. This decrease is stabilizing or even reversing in the last two decades. The CDRs show strong spatial trends in CA. Statistically significant trends in CTT are observed in global averages in the AVHRR-based CDRs, but the spatial agreement in the sign and the magnitude of the trends is weaker compared to those in CA. We also present maps of Common Stability Coverage and Common Trend Coverage that could provide a valuable metric to carry out ensemble-based analysis of the CDRs.

Author Contributions: Conceptualization, A. D.; formal analysis, A. D.; investigation, X.X.; writing—original draft preparation, A. D.; writing—review and editing, A. D. and K-G. K.; visualization, A. D.; project administration, K-G. Karlsson.; funding acquisition, A. D. and K-G. K. All authors have read and agreed to the published version of the manuscript.

Funding: This research was funded by CM-SAF/EUMETSAT and Swedish Research Council grant number 2021-05143.

Data Availability Statement: All datasets used here are publicly available through their respective data centers.
CLARA-A3 is available through: https://doi.org/10.5676/EUM_SAF_CM/CLARA_AVHRR/V003
PATMOS-x: https://www.ncei.noaa.gov/metadata/geoportal/rest/metadata/item/gov.noaa.ncdc:C00926/html
ESA Cloud CCI: https://public.satproj.klima.dwd.de/data/ESA_Cloud_CCI/CLD_PRODUCTS/v3.0/L3C/
ISCCP-HGM: https://www.ncei.noaa.gov/products/climate-data-records/cloud-properties-isccp
MODIS-Aqua: https://ladsweb.modaps.eosdis.nasa.gov/missions-and-measurements/products/MYD08_M3
CALIPSO: https://doi.org/10.5067/CALIOP/CALIPSO/LID_L3_GEWEX_Cloud-Standard-V1-00

Acknowledgments: The authors acknowledge the EUMETSAT member states for supporting CM-SAF/EUMETSAT and the science team members of all datasets used here in the study.

Conflicts of Interest: The authors declare no conflict of interest. The funders had no role in the design of the study; in the collection, analyses, or interpretation of data; in the writing of the manuscript; or in the decision to publish the results.

References

1. Tselioudis, G.; Lacis, A.A.; Rind, D.; and Rossow, W.B. Potential effects of cloud optical thickness on climate warming. Nature, 1993, 366, 670-672.
2. Bony, S.; Dufresne, J.-L. Marine boundary layer clouds at the heart of tropical cloud feedback uncertainties in climate models. Geophys. Res. Lett. 2005, 32.
3. Stephens, G. L. Cloud Feedbacks in the Climate System: A Critical Review. J. Climate, 2005, 18, 237–273, https://doi.org/10.1175/JCLI-3243.1.
4. Norris, J.; Allen, R.; Evan, A. et al. Evidence for climate change in the satellite cloud record. Nature 536, 72–75 (2016). https://doi.org/10.1038/nature18273
5. Zelinka, M. D.; Zhou, C.; Klein, S. A. Insights from a refined decomposition of cloud feedbacks. Geophys. Res. Lett. 2016, 43, 9259–9269.
6. Cesana, G.V.; Del Genio, A.D. Observational constraint on cloud feedbacks suggests moderate climate sensitivity. Nat. Clim. Change 2021, 11, 213–218.
7. Ceppi, P.; Nowack, P. Observational evidence that cloud feedback amplifies global warming. Proc. Natl Acad. Sci. 2021, 118, e2026290118.
8. Mülmenstädt, J.; Salzmann, M.; Kay, J.E. et al. An underestimated negative cloud feedback from cloud lifetime changes. Nat. Clim. Chang. 2021, 11, 508–513. https://doi.org/10.1038/s41558-021-01038-1
9. Myers, T. A., et al. Observational constraints on low cloud feedback reduce uncertainty of climate sensitivity. Nat. Clim. Change, 2021, 1-7.
10. Schiro, K.A.; Su, H.; Ahmed, F.; Dai, N.; Singer, C.E.; Gentine, P.; Elsaesser, G.S.; Jiang, J.H.; Choi, Y-S.; Neelin, J.D. Model spread in tropical low cloud feedback tied to overturning circulation response to warming, Nature Communications, 2022, 13, 1.
11. https://doi.org/10.1038/s41467-022-34787-4
12. Zelinka, M. D.; Klein, S. A.; Qin, Y.; Myers, T. A. Evaluating Climate Models' Cloud Feedbacks Against Expert Judgment. J. Geophys. Res.: Atmospheres, 2022, 127, e2021JD035198.
13. Del Genio, AD.; Kovari, W.; Yao, W.S.; Jonas, J. Cumulus microphysics and climate sensitivity. JOURNAL OF CLIMATE, 2005, 18, 2376-2387.
14. Langen, P.L.; Caballero, R. Cloud variability, radiative forcing and meridional temperature gradients in a general circulation model. Tellus A, 2007. 59:5, 641-649.
15. Klein, S.A.; Zhang, Y.; Zelinka, M.D.; Pincus, R.; Boyle, J.; Gleckler, P.J. Are climate model simulations of clouds improving? J. Geophys. Res. Atmos. 2013, 118, 1329–1342.
16. Eastman, R.; Warren, S.G. A 39-Yr Survey of Cloud Changes from Land Stations Worldwide 1971–2009: Long-Term Trends, Relation to Aerosols, and Expansion of the Tropical Belt. J. Climate, 2013, 26, 1286–1303, https://doi.org/10.1175/JCLI-D-12-00280.1
17. Rossow, W.B.; Klein, S.A.; Zhang, Y.; Zelinka, M.D.; Pincus, R.; Boyle, J.; Gleckler, P.J. Are climate model simulations of clouds improving? J. Geophys. Res. Atmos. 2013, 118, 1329–1342. Advances in understanding clouds from ISCCP. BULLETIN OF THE AMERICAN METEOROLOGICAL SOCIETY, 1999, 80, 2261-2287.
18. Wie, L.; Schumacher, C.; and McFarlane, S. A. Radiative heating of the ISCCP upper level cloud regimes and its impact on the large-scale tropical circulation, Journal of Geophysical Research: Atmospheres, 118, 2, (592-604), (2013).
19. Shepherd, T. G. Atmospheric circulation as a source of uncertainty in climate change projections. Nature Geosci. 2014, 7, 703–708.
20. Sherwood, S. C.; Bony, S.; Dufresne, J-L. Spread in model climate sensitivity traced to atmospheric convective mixing. Nature, 2014, 505, 37–42.
21. Bony, S.; Stevens, B.; Frierson, D.M.W.; Jakob, C.; Kageyama, M.; Pincus, R.; Shepherd, T.G.; Sherwood, S.C.; Siebesma, A.P.; Sobel, A.H.; et al. Clouds, circulation and climate sensitivity. Nat. Geosci. 2015, 8, 261–268.
22. Brient, F.; Schneider, T. Constraints on climate sensitivity from space-based measurements of low-cloud reflection. J. Clim. 2016, 29, 5821–5835.
23. Cronin, T.W.; Wing, A.A. Clouds, circulation, and climate sensitivity in a radiative-convective equilibrium channel model. J. Adv. Model. Earth Syst. 2017, 9, 2883–2905.
24. Ham, S.-H.; Kato, S.; Rose, F.G.; Winker, D.; L'Ecuyer, T.; Mace, G.G.; Painemal, D.; Sun-Mack, S.; Chen, Y.; and Miller, W.F. Cloud occurrences and cloud radiative effects (CREs) from CERES-CALIPSO-CloudSat-

MODIS (CCCM) and CloudSat radar-lidar (RL) products. J. Geophys. Res., 2017, 122, 8852-8884 doi: doi:10.1002/2017JD026725

25. Daloz, A. S.; Nelson, E.L.; L'Ecuyer, T.; Rapp, A.; and Sun, L. Assessing the Coupled Influences of Clouds on the Atmospheric Energy and Water Cycles in Reanalyses with A-Train Observations. J. Climate, 2018, 31, 8241–8264 doi: 10.1175/JCLI-D-17-0862.1
26. Thomas, M. A.; Devasthale, A.; Koenigk, T.; Wyser, K.; Roberts, M.; Roberts, C.; and Lohmann, K. A statistical and process-oriented evaluation of cloud radiative effects in high-resolution global models, Geosci. Model Dev., 2019. 12, 1679–1702, https://doi.org/10.5194/gmd-12-1679-2019.
27. Fueglistaler, S. Observational evidence for two modes of coupling between sea surface temperatures, tropospheric temperature profile, and shortwave cloud radiative effect in the tropics. Geophys. Res. Lett. 2019, 46, 9890–9898.
28. Zelinka, M. D.; Myers, T. A.; McCoy, D.T.; Po-Chedley, S.; Caldwell, P.M.; Ceppi, P.; Klein, S.A.; and Taylor, K.E. Causes of higher climate sensitivity in CMIP6 models, Geophys. Res. Lett., 2020, doi:10.1029/2019GL085782.
29. Rossow, W.B. 2022: History of the International Satellite Cloud Climatology Project. WCRP Report 6/2022; World Climate Research Programme (WCRP): Geneva, Switzerland, 2022, p. 87. https://doi.org/10.13021/gewex.isccp.
30. Schiffer, R.A.; Rossow, W.B. The International Satellite Cloud Climatology Project (ISCCP): The first project of the World Climate Research Programme. Bull. Am. Meteorol. Soc. 1983, 64, 779–784.
31. Heidinger, A. K.; Foster, M.J.; Walther, A.; Zhao, X. The Pathfinder Atmospheres Extended (PATMOS-x) AVHRR Climate Data Set. Bull. Amer. Meteor. Soc, 2013, doi: http://dx.doi.org/10.1175/BAMS-D-12-00246.1
32. Schulz, J.; Albert; P.; Behr H.-D.; Caprion, D.; Deneke, H.; Dewitte, S.; Dürr, B.; Fuchs, P.; Gratzki, A.; Hechler, P.; Hollmann, R.; Johnston, S.; Karlsson, K.-G.; Manninen, T.; Müller, R.; Reuter, M.; Riihelä, A.; Roebeling, R.; Selbach, N.; Tetzlaff, A.; Thomas, W.; Werscheck, M.; Wolters, E.; and Zelenka, A. Operational climate monitoring from space: the EUMETSAT Satellite Application Facility on Climate Monitoring (CM-SAF), Atmos. Chem. Phys., 2009, 9, 1687–1709, https://doi.org/10.5194/acp-9-1687-2009.
33. Karlsson, K.-G.; Anttila, K.; Trentmann, J.; Stengel, M.; Meirink, J.F.; Devasthale, A.; Hanschmann, T.; Kothe, S.; Jääskeläinen, E.; Sedlar, J.; et al. CLARA-A2: The second edition of the CM SAF cloud and radiation data record from 34 years of global AVHRR data. Atmos. Chem. Phys. 2017, 17, 5809–5828.
34. Stengel, M., Stapelberg, S., Sus, O., Schlundt, C., Poulsen, C., Thomas, G., Christensen, M., Carbajal Henken, C., Preusker, R., Fischer, J., Devasthale, A., Willén, U., Karlsson, K.-G., McGarragh, G. R., Proud, S., Povey, A. C., Grainger, R. G., Meirink, J. F., Feofilov, A., Bennartz, R., Bojanowski, J. S., and Hollmann, R. Cloud property datasets retrieved from AVHRR, MODIS, AATSR and MERIS in the framework of the Cloud_cci project, Earth Syst. Sci. Data, 2017, 9, 881–904, https://doi.org/10.5194/essd-9-881-2017.
35. Platnick, S.; Meyer, K.G.; King, M.D.; Wind, G.; Amarasinghe, N.; Marchant, B.; Arnold, G.T.; Zhang, Z.; Hubanks, P.A.; Holz, R.E.; et al. The MODIS Cloud Optical and Microphysical Products: Collection 6 Updates and Examples from Terra and Aqua. IEEE Trans. Geosci. Remote Sens. 2017, 55, 502–525. https://doi.org/10.1109/TGRS.2016.2610522.
36. Stephens, G.; Winker, D.; Pelon, J.; Trepte, C.; Vane, D.; Yuhas, C.; L'Ecuyer, T., and Lebsock, M.. CloudSat and CALIPSO within the A-Train: Ten years of actively observing the earth system, B. Am. Meteorol. Soc., 2018. 99, 569–581, https://doi.org/10.1175/BAMS-D-16-0324.1
37. Karlsson, K.-G.; Devasthale, A. Inter-Comparison and Evaluation of the Four Longest Satellite-Derived Cloud Climate Data Records: CLARA-A2, ESA Cloud CCI V3, ISCCP-HGM, and PATMOS-x. Remote Sens. 2018, 10, 1567.
38. Stubenrauch, C.J.; Rossow, W.B.; Kinne, S.; Ackerman, S.; Cesana, G.; Chepfer, H.; Di Girolamo, L.; Getzewich, B.; Guignard, A.; Heidinger, A.; et al. Assessment of global cloud datasets from satellites: Project and Database initiated by the GEWEX Radiation Panel. Bull. Am. Meteorol. Soc. 2013, 23, 1031–1049. https://doi.org/10.1175/BAMS-D-12-00117.1.
39. Karlsson, K.-G.; Stengel, M.; Meirink, J.F.; Riihelä, A; Trentmann, J.; Akkermans, T.; Stein, D.; Devasthale, A.; Eliasson, S.; Johansson, E.; et al. CLARA-A3: The third edition of the AVHRR-based CM SAF climate data record on clouds, radiation and surface albedo covering the period 1979 to 2023. Earth Syst. Sci. Data Discuss. 2023, In Review. https://doi.org/10.5194/essd-2023-133.
40. Stengel, M.; Stapelberg, S.; Sus, O.; Finkensieper, S.; Würzler, B.; Philipp, D.; Hollmann, R.; Poulsen, C.; Christensen, M.; McGarragh, G. Cloud_cci Advanced Very High Resolution Radiometer post meridiem

(AVHRR-PM) dataset version 3: 35-year climatology of global cloud and radiation properties. Earth Syst. Sci. Data 2020, 12, 41–60, https://doi.org/10.5194/essd-12-41-2020.

41. Foster, M.J.; Phillips, C.; Heidinger, A.K.; Borbas, E.E.; Li, Y.; Menzel, W.P.; Walther, A.; Weisz, E. PATMOS-x Version 6.0: 40 Years of Merged AVHRR and HIRS Global Cloud Data. J. Clim. 2022, 36, 1143–1160. https://doi.org/10.1175/JCLID-22-0147.1.
42. Young, A.H.; Knapp, K.R.; Inamdar, A.; Hankins, W.; Rossow, W.B. The International Satellite Cloud Climatology Project H-Series climate data record product. Earth Syst. Sci. Data 2018, 10, 583–593.
43. Xiong, X.; Butler, J.J. MODIS and VIIRS Calibration History and Future Outlook. Remote Sens. 2020, 12, 2523. https://doi.org/10.3390/rs12162523
44. The 2022 GCOS ECV requirements: GCOS-245, 2022, pp 1-244 available at: https://library.wmo.int/index.php?lvl=notice_display&id=22135
45. Karlsson, K.-G.; Håkansson, N. Characterization of AVHRR global cloud detection sensitivity based on CALIPSO-CALIOP cloud optical thickness information: demonstration of results based on the CM SAF CLARA-A2 climate data record. Atmos. Meas. Tech. 2018, 11, 633–649, https://doi.org/10.5194/amt-11-633-2018.
46. Karlsson, K.-G.; Devasthale, A.; Eliasson, S. Global Cloudiness and Cloud Top Information from AVHRR in the 42-Year CLARA-A3 Climate Data Record Covering the Period 1979–2020. Remote Sens. 2023, 15, 3044. https://doi.org/10.3390/rs15123044
47. Håkansson, N.; Adok, C.; Thoss, A.; Scheirer, R.; Hörnquist, S. Neural network cloud top pressure and height for MODIS. Atmos. Meas. Tech. 2018, 11, 3177–3196, https://doi.org/10.5194/amt-11-3177-2018.
48. Devasthale, A., Karlsson, K.-G., Quaas, J., and Grassl, H.: Correcting orbital drift signal in the time series of AVHRR derived convective cloud fraction using rotated empirical orthogonal function, Atmos. Meas. Tech., 5, 267–273, https://doi.org/10.5194/amt-5-267-2012, 2012.
49. Evan AT, Heidinger AK, Vimont DJ, 2007: Arguments against a physical long-term trend in global ISCCP cloud amounts. Geophysical Research Letters 34:4